

# Contribution in the Study and Numerical Investigation of the Flow Characteristics in a Solar Chimney

<sup>1</sup>Khaled Mahdi, <sup>2</sup>Nadir Bellel

<sup>1</sup>Hydrometeorological Institute for Training and Research Oran, Algeria

<sup>1,2</sup>Energy Physics Laboratory, University of Mentouri, Constantine 1, Algeria

e-mail: khaled\_mahdi@yahoo.fr; bellelnadir@yahoo.fr

**Abstract.** In this present work, the power generation performance in a solar chimney system (SCS) was investigated using computational fluid dynamics (CFD). The main objective of this study is to examine the impact of the chimney shape in the power output of a SCS. The mathematical model mentioned below was solved by the commercial CFD FUEENT 6.3. The model is validated by experimental results from the literature review and used as predictive tool. The influence of the absorber temperature, the geometrical shapes of the solar chimney system on the power output of the SCS. These results lead to the better understanding of the impact on these parameters on the thermal updraft wind SCS operating system.

## 1. Introduction

The solar chimney system (SCS) converts solar energy into mechanical energy and then using a wind turbine /generator, this mechanical energy converted into electrical energy. The system uses the greenhouse effect in the collector to generate updraft in the chimney, which can drive wind turbines for electricity production. SCS has advantages in its low cost of construction and function, and the supply of renewable energy to communities without aggravating environmental pollution and intensifying climate change. SCS is considered to have high potential for application in developing countries with extensive available field and abundant solar isolation. The solar chimney power plant concept was originally proposed in 1903 by Isidoro Cabanyes [1]. In 1931, a description of a solar chimney power plant was presented by Günther [2].

The basic study on the solar chimney concept was performed by Schlaich in the 1970, and in 1981 he began the construction of a 50kW pilot solar chimney power plant in Manzanares, Spain [2], [3]. Studying the impact of different components in a solar chimney is a primary task for designing a solar chimney power plant. Haaf *et al.* [3], [4] indicated that the critical roles of chimney height and air temperature in determining the system power output. Pasumarthi *et al.* [4], [5] established a mathematical model for estimating the heat transferring process and the airflow in a SCS.

## 2. Experimental Setup

The basic dimension of the SCS was built in Wind Engineering Section at Kyushu University research institute for applied mechanics (RIAM) Japan [6] are as follows:

Chimney height for cylindrical and conic shape, 2 m; chimney radius, 0.16 m; collector radius, 1.5 m; height between the inlet of the collector and the center, 0.2 m (as shown in Figure 1).



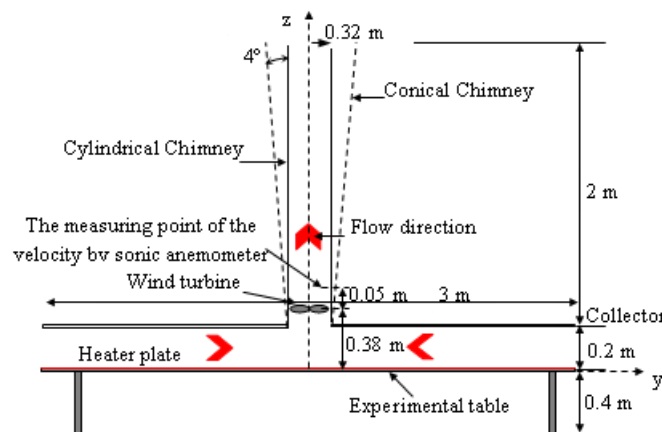


Figure 1. Schematic diagram of a SCS.

### 3. CFD Simulation Methods

The solar chimney geometry was created using GAMBIT (Version 2.4.6), the pre-processing module of the FLUENT (Version 6.3.26) code. The schematic appearance of the different shape of the chimney is shown in Figure 2. The following two assumptions have been made:

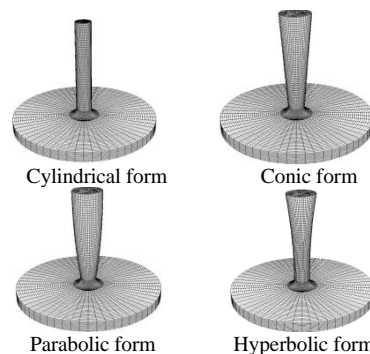


Figure 2. Three-dimensional view of the different shapes solar chimney.

- 1) The absorber surface of the collector is assumed to be uniform and smooth.
- 2) The temperature of the absorber surface of the collector is assumed the same.

In actual condition of the absorber temperature of the collector, a temperature difference exists between the middle and the edge of the absorber. The air temperature variation exists of the edge at the center of the absorber caused by the surrounding environment of the experiment. This is because of the natural convection heat loss from the chimney aperture to the ambient. Therefore, in the present numerical analysis a temperature difference ( $\Delta T$ ) of 20°C to 40°C has been considered between absorber surface and ambient temperature of the laboratory. The total numbers of cells has been fixed approximately 860725 tetrahedral cells. The grid generation for computational domain is shown in Figure 1.

#### 3.1. Numerical Procedure

Four different chimney shapes: cylindrical, conic, parabolic and hyperbolic are investigated in this study. Each form is modelled as show in Figure 2 using the Gambit tool of Fluent CFD software package [7]. The geometry and mesh were created using GAMBIT 3. and duplicating the actual geometry of the different chimney form. For modelling a solar chimney, The 3D modelling and grid generation was carried out in the GAMBIT 2.0.4 package.

#### 3.2. Numerical Solution

The basic equations including the models discussed till now were numerically solved with the help of the commercial simulation program FLUENT (version 6.23). Fluent uses the finite volume method for the solution of the differential equations. The basic equations were solved numerically with the help of the SIMPLE algorithm (Semi-Implicit Method for Pressure-Linked-Equations). The accuracy of all approximations was second order. The standard relaxation parameters were adapted for this. Many cells in the radial direction and relatively few in the x direction are used in the collector of the upwind power plant. The reverse is valid in the chimney. All numerical calculations had to be carried out with the solver with double precision. A convergence criterion of  $10^{-3}$  was imposed on the residuals of the continuity equation momentum equation. The convergence criterion  $10^{-6}$  was given on the residual of energy equation. A typical numerical simulation process is described in Figure 3.

TABLE I. BOUNDARY CONDITIONS AND MODEL PARAMETERS RADIATION PROPERTIES OF WALL

materials	$\alpha$	$\rho$	$\tau$
Glass	0.06	0.95	0.84
Absorber plat	0.95	0.95	0

### 3.3. Mathematical Model and Boundaries Conditions

Since the purpose of this numerical study is to understand the flow characteristics and the effect of the geometry on the solar chimney performance that was built in RIAM, not the assessment of turbulence models, it is decided that a standard k- $\epsilon$  model [8] would serve the purpose which is also adopted by Motoyama *et al.* and Sangi *et al.* [9], [10]. The conservation equations and the standard k- $\epsilon$  turbulent model used in this study is shown below:

The continuity equation:

$$\frac{\partial u_i}{\partial x_i} = 0 \quad (1)$$

Conservation of momentum is described by:

$$\frac{\partial u_i}{\partial t} + u_i \frac{\partial u_i}{\partial x_i} = -\frac{1}{\rho} \frac{\partial p}{\partial x_i} + \nu \frac{\partial^2 u_i}{\partial x_j \partial x_j} + \rho f_i \quad (2)$$

where  $p$  is the static pressure,  $\nu \frac{\partial^2 u_i}{\partial x_j \partial x_j}$  is the stress tensor (described below), and  $\rho f_i$  is the gravitational body force and external body forces.

The energy equation in the following form:

$$\frac{\partial(\rho c_p T)}{\partial t} + \frac{\partial(\rho u_j c_p T)}{\partial x_j} = \frac{\partial}{\partial x_j} \left( \lambda \frac{\partial T}{\partial x_j} \right) + T \beta \frac{\partial p}{\partial t} + S_h \quad (3)$$

For the standard k- $\epsilon$  models, the constants have the following values [10]:

$$C_{1\epsilon}=1.44, C_{2\epsilon}=1.92, C_\mu=0.09, \sigma_k=1.0, \sigma_\epsilon=1.3. \quad (4)$$

### 3.4. Boundary Conditions

The boundary conditions such as absorber collector and ambient temperature are defined from the laboratory conditions [11], [12], [13]. The relative static pressure of the collector inlet is zero, and the temperature is the ambient temperature:

$$P_{\text{int}} = 0, \quad \text{and} \quad T_{\text{int}} = T_\infty \quad (5)$$

$$\text{by:} \quad \frac{\partial T}{\partial x} = 0, \quad u = 0, \quad v = 0 \quad (6)$$

The above relations express an adiabatic wall and the non-slip conditions respectively.

Data for an acrylic sheet and absorber plate in terms of optical factor is illustrated in Table II.

TABLE II. PHYSICAL PROPERTIES OF WALLS OF THE SOLAR CHIMNEY PROTOTYPE

materials	$\alpha$	$\rho$	$\tau$	$\rho(\text{kg}/\text{m}^3)$	$C_p(\text{J/kg}/\text{K})$	$\lambda(\text{W/m}/\text{K})$
acrylic sheet	0.06	0.95	0.84	1190	1465	0.19
Absorber plate	0.95	0.95	0	7830	491	70

### 3.5. Numerical Method Validation

In order to validate our numerical method, we performed a numerical study using the Japanese prototype data for the experience at laboratory used by the validation reference work (Haaf, 1984). Transient numerical results for the fluid motion established in the Japanese prototype are presented, including the required validation with appropriate experimental results. The numerical results for the air temperature at the inlet section of the wind turbine, during the whole day, follows the same trend as the experimental results of Japanese [5], with an average deviation of 12% (Figure 3). The results obtained for the air velocity in the same section are shown in Figure 4. On the same figure, values measured just prior 8:00 and around 20:00 are discarded (the respective rapid increase and decrease reached in the stack effect can be due to external atmospheric agents). The average deviation is, at most, equal to 12%. It can be observed, on figure 10, the expected power from the present simulation and the one given by Haaf (1984). We notice the same trend and an average deviation of around 9%.

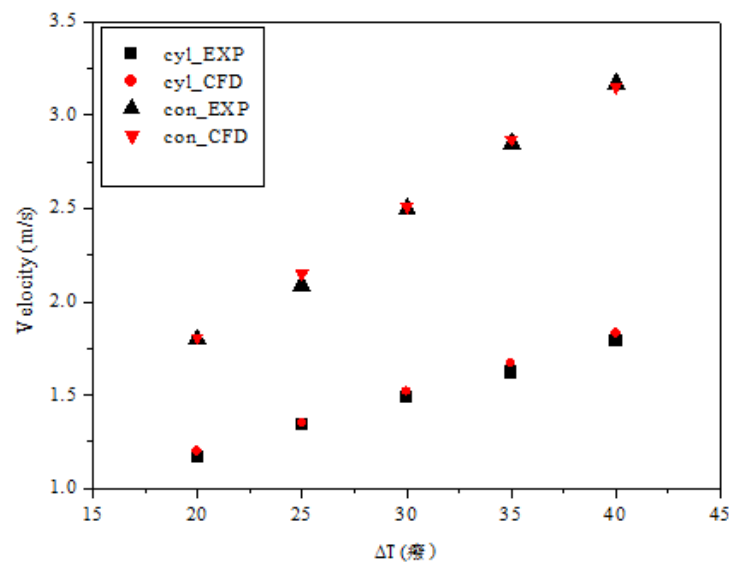
Figure 3. Comparison of velocity between CFD model and experimental data at  $y=0.38$  m.

TABLE III. CURVE FITTING IN THE CYLINDRICAL AND CONICAL CHIMNEY AND THE PREDICTION OF OPTIMAL GEOMETRY

Curve equation	$u = A + B \times \Delta T$			
	cyl_EXP	Cyl_CFD	con_EXP	Con_CFD
A	0.570	0.566	0.382	0.458
B	0.030	0.031	0.070	0.068
$R^2$	0.99905	0.99984	0.99883	0.99915

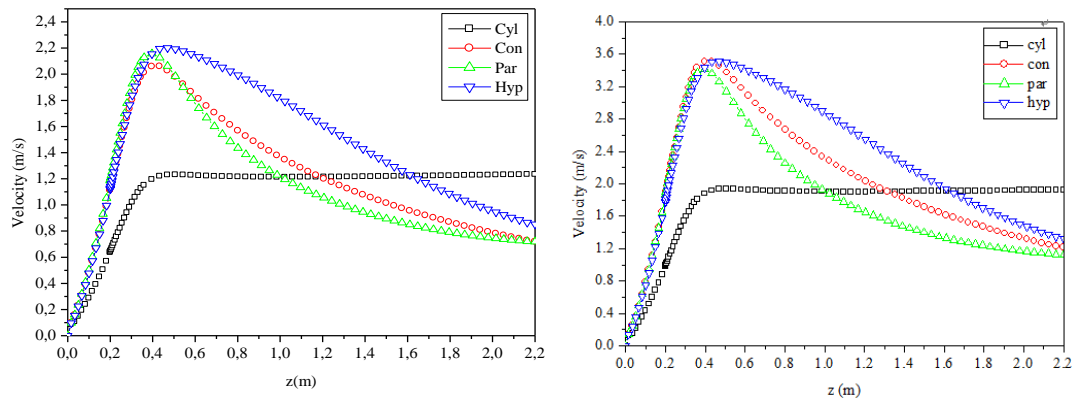


Figure 4. Effect of the chimney shapes on the updraft velocity,  $\Delta T = 20^\circ\text{C}$  and  $40^\circ\text{C}$ .

Figure 4 and Figure 5 shows the velocity updraft, through the height of the chimney. We notice that velocities in the three shapes (cylindrical, conic, parabolic and hyperbolic) increase regularly with increasing temperature difference between absorber plate and ambient temperature.

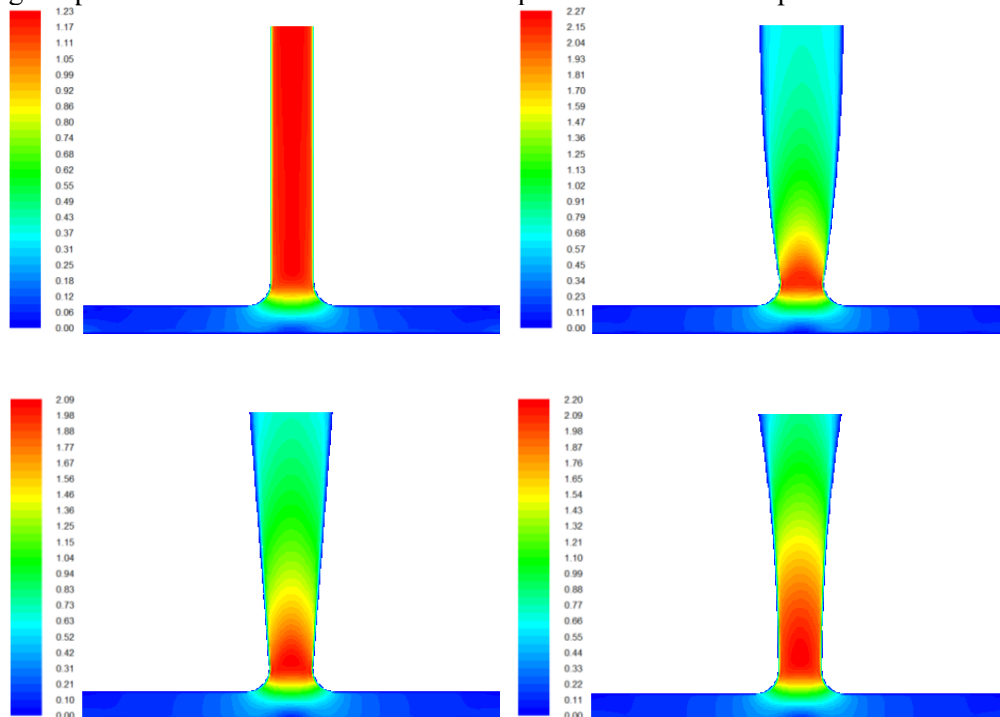


Figure 5. Profiles of air velocity through the chimney for different shapes of chimney,  $\Delta T = 20^\circ\text{C}$ .

We see in Figure 6 and 7 the temperature is decreased because airflow is rising in the chimney as show in Table III. The temperature rapidly falls because of the velocity updraft of three forms (conic, parabolic and hyperbolic) compared from cylindrical shape, because as hot air rises with important velocity updraft, air temperature rapidly falls; outer portion of the chimney is insulated from four shapes. Air velocity in collector was slow due to larger height (0.2 m) compared of the chimney radius. In addition, at the point of  $z = 0.38\text{ m}$  and it rises rapidly at the point  $z = 0.5\text{ m}$  due to the sudden contraction in chimney sections.

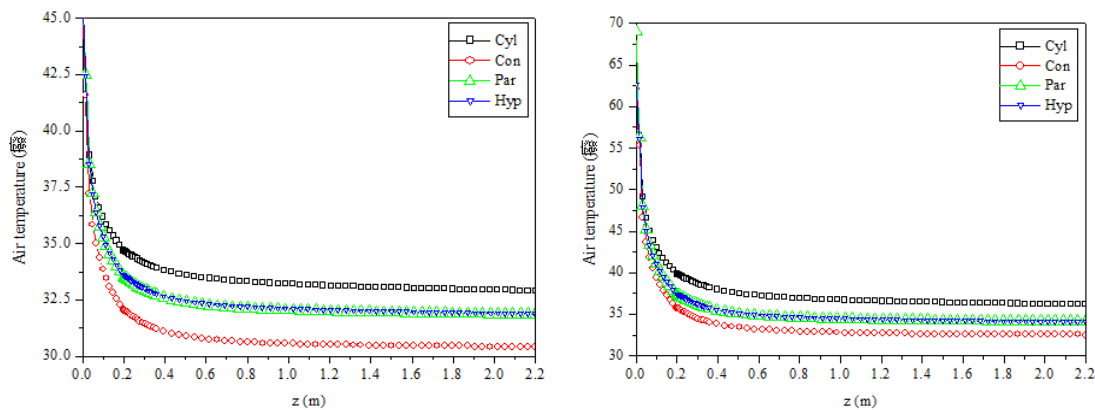
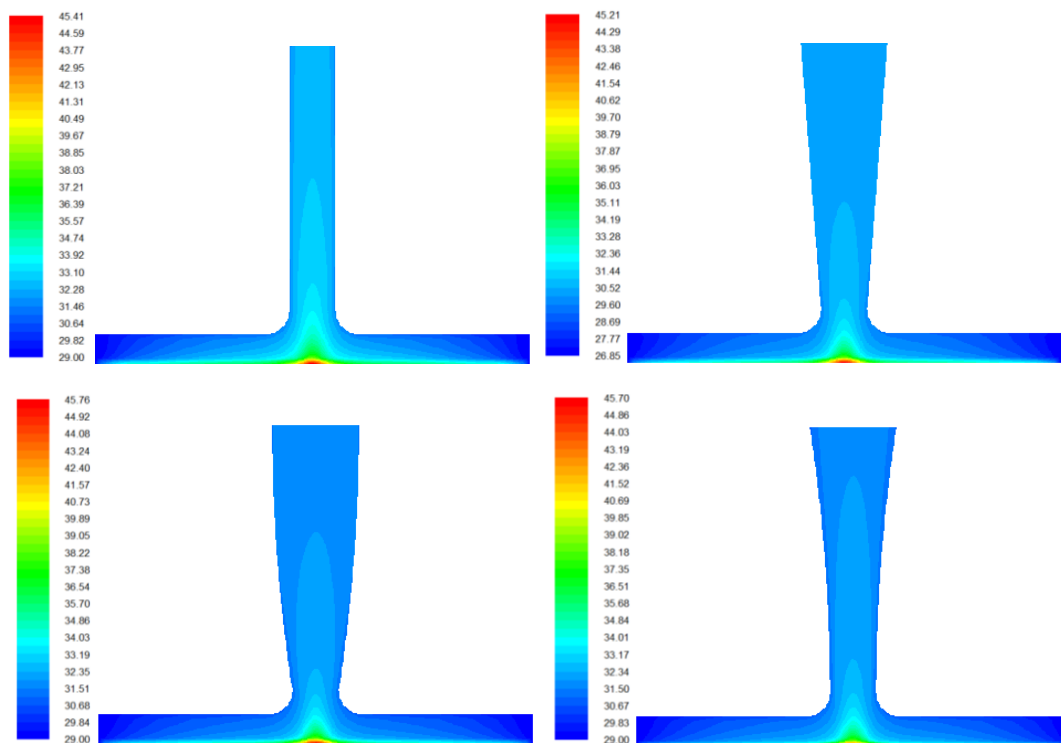
Figure 6. Effect of the chimney shapes on the updraft velocity,  $\Delta T=20\text{ }^{\circ}\text{C}$  and  $40\text{ }^{\circ}\text{C}$ Figure 7. Profiles of air temperature through the chimney for different shapes of chimney,  $\Delta T=20\text{ }^{\circ}\text{C}$ .

Table IV shows that the maximum velocity is occurring inside the chimney at different levels, same for Power out and comparative obtained by CFD simulation up to 0.7m of th height.

TABLE IV. COMPARISON BETWEEN THE AIR VELOCITIES OBTAINED BY CFD SIMULATION

chimney	z (m)	$u_{\max}$ (m/s)	$\bar{u}$ (m/s)	$P_{\max}$ (mW)	$\dot{m}$ (kg/s)	ratio
cyl	0.50	1.87	1.82	22.68	0.1651441	1
con	0.39	3.44	2.43	141.26	0.3182465	4.74
par	0.36	3.38	2.18	134.72	0.3182036	4.12
hyp	0.43	3.39	2.70	135.42	0.3019360	5.63

#### 4. Conclusion

The investigation of the velocity updraft from solar chimney shapes was undertaken numerically and was validated using the published experimental results for two different chimneys geometries

(cylindrical and conical shape). A good agreement between experimental and numerical results was obtained, it is determined that due to the shape of chimney is affected, performance of the system increases positively. In the conclusion, one can say that the shape of the conical, parabolic and hyperbolic chimney gives almost the same maximum available power compared with cylindrical shape of the SCS.

We have obtained:

- The available power of the SCS increases with increases of the absorber plate temperature differences.
- The main power available of the hyperbolic SCS is five times greater than the cylindrical SCS.

### Nomenclature

Symbol	Nom,	unit é
A	area,	$m^2$
k	kinetic energy of turbulence,	$m^2/s^2$
T	temperature,	K
u	velocity ,	m/s
$\bar{u}$	mean velocity,	m/s
z	chimney height,	m
$\dot{m}$	mass rate,	kg/s
Cp	power coefficient	
p	pressure,	pa
R	correlation coefficient	
<b>Greek letters</b>		
$\alpha$	absorptivity	
$\rho$	Reflectivity	
$\tau$	transmittivity	
$\varepsilon$	rate of dissipation,	$m^2/s^2$
$\beta$	thermal expansion coefficient	1/K
$\delta_{ij}$	kronicer symbol	
$\infty$	ambient	
<b>Acronym</b>		
cyl	cylindric	
con	conic	
par	parbolic	
hyp	hyperbolic	
EXP	experimental	
CFD	computational fluid dynamics	
RIAM	research institute for applied mechanics	

### 5. References

- [1] J. Lorenzo, Las Chimneas solares: de una propuesta espanola en 1903 a de Manzanares, <http://www.fotovoltica.com/chimenea.pdf>.
- [2] H. Günther, Hundred Years-Future Energy Supply of the World, Franckhsche Verlagshandlung, Stuttgart, Germany, 1931.
- [3] W. Haaf, "Solar chimneys, part II: preliminary test results from the Manzanares pilot plant," International Journal of Solar Energy, vol. 2, May.1984, pp. 141-161,doi:10.1080/01425918408909921
- [4] W. Haaf, K. Friedrich, G.Mayr, and J. Schlaich, "Solar chimneys, part I: principle and construction of the pilot plant in Manzanares," International Journal of Solar Energy, vol 2, Apr. 1983, pp. 3-20,doi: 10.1016/B978-0-12-384988-5.00032-2
- [5] S. W.Yuan, "Foundations of Fluid Mechanics", 3<sup>rd</sup> ed., Prentice Hall International, London, pp. 104-113, 1988.
- [6] Fluent 6.2 user guide, Fluent, Inc., Lebanon, NH, 2004.
- [7] M. Motoyama, K. Sugitani, Y. Ohya, T. Karasudani, T. Nagai and S. Okada, "Improving the power generation performance of a solar tower using thermal updraft wind," Energy Power

- Eng, vol. 6, Sep. 2014, pp. 362-370, doi: 10.1145/566654.566623
- [8] M. Motoyama, K. Sugitani, Y. Ohya, T. Karasudani, T. Nagai And S.Okada, "Improvement of power generation on solar tower by thermal updraft wind", 23<sup>rd</sup> Conference Wind Engineering , 2014, doi: 10.14887/kazekosymp.23.0\_109
- [9] R. Sangi, M. Amidpour and B. Hosseinizadeh, "Modelling and numerical simulation of solar chimney power plants," Sol Energy, vol.85, 2011, pp. 829-838, doi: 10.1145/566654.566623
- [10] T. Ming, W. Liu and G. Xu , "Analytical and numerical investigation of the solar chimney power plant systems," Int. J. Energy Res, vol. 30, Apr. 2006, pp. 861–873, doi: 10.1002/er.1191
- [11] B.E. Launder and D.B. Spalding, "The numerical computation of turbulent flows," Comput Methods Appl. Mech Eng, vol. 3, March. 1974, pp. 269–289, doi: 10.1016/0045-7825(74)90029-2
- [12] M.O. Hamdan and O. Rabbata, "Experimental Solar Chimney Data with Analytical Model Prediction," in Proceedings of the Solar Conference, vol. 1, pp. 327-332. World Renewable Energy Forum, WREF2012, ISBN:9781622760923, Denver, Colorado, 13–18 May 2012.
- [13] Fluent CFD software package, version 6. 3. 26, 2006.